GA–A26784

TWO DIMENSIONAL TRANSPORT EFFECTS IN THE TOKAMAK SCRAPE-OFF LAYER PLASMA

by

D.N. HILL, G.D. PORTER, and T.D. ROGNLIEN

JULY 2010

GENERAL ATOMICS

DISCLAIMER

GA–A26784

TWO DIMENSIONAL TRANSPORT EFFECTS IN THE TOKAMAK SCRAPE-OFF LAYER PLASMA

by
D.N. HILL,* G.D. PORTER,* and T.D. ROGNLIEN*

This is a preprint of a paper to be presented at the Nineteenth International Conference on Plasma Surface Interactions, May 24-28, 2010, in San Diego, California, and to be published in the *Proceedings.*

*Lawrence Livermore National Laboratory, Livermore, California.

Work supported by
the U.S. Department of Energy
under DE-FC02-04ER54698 and DE-AC52-07NA27344

GENERAL ATOMICS PROJECT 30200
JULY 2010

GENERAL ATOMICS

ABSTRACT

The effect of 2D transport in the tokamak scrape-off layer (SOL) on relating measured divertor heat flux profiles to midplane plasma profiles is explored with the UEDGE code for a range of transport assumptions. The relationship between the divertor heat flux profile and the midplane plasma temperature profile as determined from UEDGE is compared to commonly used predictions from 1D and "2-point" analytic relation. Results show that the parametric variation in $\lambda_{q,div}$ with midplane separatrix values follows the conduction-limited 2-point model, though the actual valuate of $q_{//}$ on a given flux surface is much lower than implied by the midplane $T_{e,sep}$, and $\lambda_{q,div}$ is ~ twice as wide as expected from these models. Poloidal variations in χ result in minimal change to radial profiles and probably can't be distinguished experimentally from cases with uniform χ having the same flux-surface average value.

I. INTRODUCTION

The prediction of peak steady-state heat loads on divertor surfaces is an important element for the design of next generation tokamak burning plasma fusion experiments. Predictions can be based on extrapolation from existing measurements and/or numerical simulations which incorporate relevant scrape-off layer (SOL) physics. Due to the complexity of simulations which accurately treat the SOL geometry and the broad range of relevant physical effects, trends in experimental data are often compared against simple 1D or 1.5D analytic approximations.

In this paper we use the UEDGE 2D scrape-off layer simulation code [1] to examine how well the simple models reproduce the properties of the SOL plasma as determined by the more complete treatment. At the same time, we examine the scaling of peak divertor heat flux and profile width with upstream parameters such as electron temperature, power, density, toroidal field (connections length) and transport coefficients. The purpose of this activity is not to evaluate the validity of UEDGE in matching experiment as in [2-4], but rather to use it as a tool to understand the effect of the 2D geometry as it impacts the behavior of the SOL for only the simplest of effects; namely, thermal transport in the absence of large radiative losses, high impurity concentrations, strong flows, and transients.

In the following sections we examine several aspects of SOL thermal transport, first summarizing basic transport equations and the assumptions that result from considering parallel thermal transport as “dominant.” Then, UEDGE is used to compute basic SOL parameters and the UEDGE output is compared to the simple model. Finally, the effects of the 2D divertor tokamak geometry and of spatially varying transport coefficients are examined.

II. THE SOL DOMINATED BY PARALLEL THERMAL CONDUCTION

It is well known that the heat conduction along magnetic field lines is much larger than cross-field thermal conduction [5,6]. At $n_{e,mid} = 2\times10^{19}$ m^{-3} and $T_{e,mid} = 100$ eV with $\chi_e = 1$ m^2/s, parallel and perpendicular power densities are 1.0×10^9 and 6.4×10^4 (W/m^2), for 20 m and 0.5 cm gradient scale lengths, respectively. Parallel thermal conductivity is independent of density, but depends strongly on temperature $\left(T^{3/2}\right)$, while perpendicular conductivity depends on the product of density (n) times the anomalous radial thermal diffusivity for ions (electrons), $\chi_{e,i}$. For electrons, the relations are [5]:

$$q_{\parallel}\left(W/\mathrm{m}^2\right) = -2050T_e^{5/2}\frac{dT_e(\mathrm{eV})}{ds(\mathrm{m})} \quad , \tag{1}$$

for $Z = 1$, and

$$q_{\perp,e}\left(W/\mathrm{m}^2\right) = 3200n\left(10^{20}\ \mathrm{m}^{-3}\right)\chi_e\left(\mathrm{m}^2/\mathrm{s}\right)\frac{dT_e(\mathrm{eV})}{dy(c\mathrm{m})} \quad , \tag{2}$$

where s is the distance along field lines and y is the distance perpendicular to a flux surface. While the ratio of parallel to perpendicular power density is large, the total plasma surface area on the separatrix is much larger (~25 m^2 in the DIII-D tokamak) than the cross sectional area of the SOL perpendicular to **B** (0.017 m^2), so both components are important on a flux surface.

Frequently, for qualitative scaling purposes, the radial transport on a flux tube is neglected, so the energy balance can be integrated along field lines, giving the well-known relationship between upstream and downstream electron temperatures for plasmas subject to collisional thermal conduction,

$$q_{\parallel} = \left(T_{e,mid}^{7/2} - T_{e,div}^{7/2}\right)\Big/L_{\parallel} \quad . \tag{3}$$

Given the large exponent, the downstream temperature can be neglected. If this relationship holds on flux surfaces, the ratio of the heat flux to electron temperature scale lengths immediately follows: $\lambda_{q,mid} \propto {}^{2}\!/\!_{7}\,\lambda_{T,mid}$, with the divertor heat flux related to the midplane heat flux by magnetic flux expansion.

The integrated 1D model can be expanded by including integrated radial energy transport in the entire SOL, thereby finding the overall *e*-folding width of the SOL at the midplane, $\lambda_{q,mid}$,

$$\lambda_{q,mid} \propto \frac{q_{95}^{4/9} \quad n_{e,mid}^{7/9} \quad \chi_{\perp}^{7/9}}{P_{SOL}^{7/9}} \quad , \tag{4}$$

where q_{95} is the safety factor at the 95% flux surface. This is the so-called 2-point SOL model, as discussed in Ref. 2. When the parallel heat flux is limited by the sheath at the divertor plate, the divertor temperature is not much lower than the midplane temperature, and a much weaker dependence on density and power results

$$\lambda_{q,mid} \propto \frac{q_{95}^{2/5} \quad n_{e,mid}^{1/5} \quad \chi_{\perp}^{3/5}}{P_{SOL}^{1/5}} \quad . \tag{5}$$

These relations will now be compared with UEDGE simulations.

III. UEDGE SIMULATION METHODOLOGY

The UEDGE code solves the 2D transport equations for particles (fuel and impurity ions), momentum, and energy on a 50 × 30 mesh (poloidal x radial) spanning the edge plasma from 3 cm inside the separatrix to 1.8 cm outside the separatrix at the plasma midplane. The UEDGE code calculates the ionization source and radiative and charge exchange losses throughout the plasma. Flux limits to ion and electron parallel thermal conductivity were enabled, but neither particle drifts nor impurity transport were turned on for this study. The calculated divertor heat flux includes electron and ion conduction, convection, classical sheath physics, and recombination energy [2].

The computational mesh was generated from DIII-D MHD equilibria provided by EFIT. Thomson scattering data from lower-single-null discharges used in a divertor experiment provided initial starting point for the density (134079 through 134082) at the top of the pedestal; the total power from the core plasma was set equal to the neutral beam heating power. The plasma shape was nearly identical for these discharges.

Scans with UEDGE were carried out by varying only the single parameter of interest rather than trying to mimic or match how all the midplane parameters vary when one parameter is changed. Once the run was complete, all relevant quantities were available for plotting and analysis, making it a simple matter to determine gradient scale lengths as a function of position in the SOL, which then could be used to evaluate Eqs. (4), (5), and (6). In all, over 50 UEDGE runs were completed, which included scans of power, density, toroidal field, carbon impurity fraction/radiative loss, and radial transport coefficients.

IV. ANALYSIS OF POWER BALANCE ON SOL FLUX SURFACES

Power flows into the tokamak SOL through radial transport across the whole plasma separatrix surface, whereas the basic analysis of Eqs. (4)-(6) assumes that power flows into the SOL at a single location. As the full 2D UEDGE simulation shows, the immediate consequence is that Eq. (4) no longer strictly applies globally in the SOL, and so knowing the midplane electron temperature does not directly specify the parallel heat flux on a flux surface. Figure 1 shows that the poloidal distribution of the perpendicular heat flux across the separatrix into the SOL $\left(q_{\perp}\right)$ is strongly peaked at the outboard midplane (defined as $\theta_{pol} = 270°$) due to the radial compression of flux surfaces there, even when the radial transport (χ_e and χ_i) is spatially uniform. Further, the parallel heat flux does not peak at the same place as $q_{\perp,}$ but down near the x-point, closer to the divertor targets, and there is a stagnation point (zero parallel heat flux) near the top of the plasma, opposite the x-point. Yet, as shown, the electron temperature in the SOL remains high around the whole boundary.

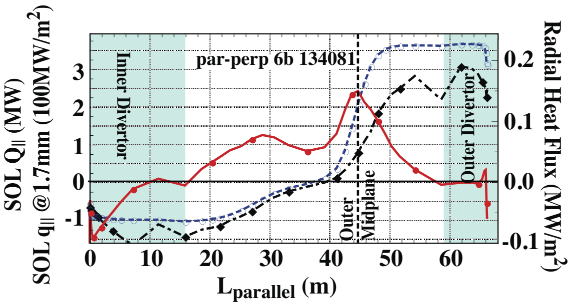

Fig. 1. Poloidal distribution of parallel and perpendicular heat flux into the SOL as a function of parallel length along a field line 1.7 mm outside separatrix: total parallel energy flux $Q_{||}$ (○ dashed), parallel heat flux $q_{||}$ (◆) on 1.7 mm field line, and radial heat flux $q_{\perp}$ across separatrix (● solid). Inboard midplane is at L=28.8 m.

Another effect also comes into play which further breaks the relation between downstream heat flux (near the divertor targets) and midplane T_e implied by Eq. (4). Radial transport removes energy from higher temperature flux surfaces to neighboring, cooler flux surfaces further out in the SOL. For example, with $\chi_e = 0.5\ \mathrm{m}^2/\mathrm{sec}$ (a common value derived from fitting T_e profiles in DIII-D H-mode discharges), half the power crossing the separatrix is transported radially outward from the first 2 mm of the SOL, leaving only half to arrive at the divertor target. In Fig. 2 we plot the heat flux at the outer divertor target as determined from UEDGE (2D solution) and the heat flux as determined from Eq. (4) using $T_{e,mid}$ from UEDGE vs the radial distance from the separatrix strike point. As shown, the actual divertor heat flux across the SOL is only about 30% of that implied by the simple 1D analysis. This ratio is fairly independent of χ_e in the SOL.

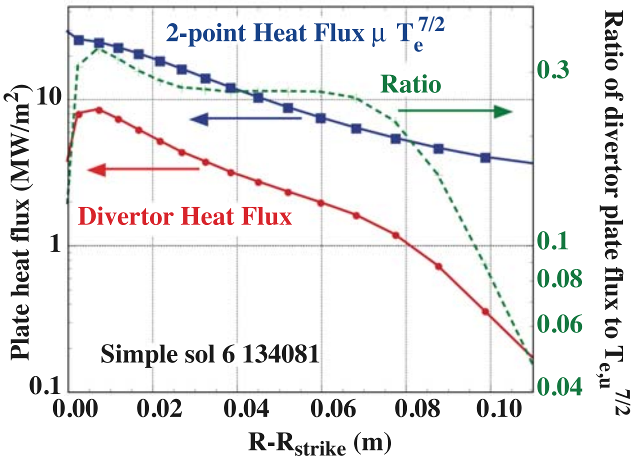

Fig. 2. Outer-leg divertor heat flux profiles from UEDGE (•), Eq. (5) (○), and their ratio (▲).

Below the x-point, additional energy loss from flux tubes occurs by radial transport into the private flux region (PFR). The effect is not as large as might be imagined considering that the private region has no source of energy, because magnetic flux expansion is large near the x-point, reducing the radial temperature gradient. For typical DIII-D divertor configurations, UEDGE predicts only about 10-12% of the outer-divertor SOL power diffuses into the PFR, and reducing χ_e nearly to zero in the private region reduces this fraction to just less than 10%, with a corresponding rise in peak heat flux of less than 20%.

V. RELATIONSHIP BETWEEN MIDPLANE TEMPERATURE PROFILES AND DIVERTOR HEAT-FLUX PROFILES

The large uncertainties in the divertor heat flux database for ITER, as well as projections of very high heat flux for DEMO, have motivated increased interest in quantifying the dependence of the divertor heat flux profile width on core plasma parameters and upstream/midplane SOL temperature profiles [7]. Figure 3 shows that the full $1/e$ width of the outer divertor heat flux profile, when mapped back to the midplane, is nearly a factor of two larger than the electron temperature e-folding length $\lambda_{q,mid}/\lambda_{T,mid}=0.6$, as compared to 2/7=0.28). Here we have computed the slope of the temperature profile over the range 0 to 0.4 cm just outside the separatrix, in the region where the divertor heat flux peaks and begins to fall off. As shown, the ratio $\lambda_{q,mid}/\lambda_{T,mid}$ is relatively insensitive to χ_e.

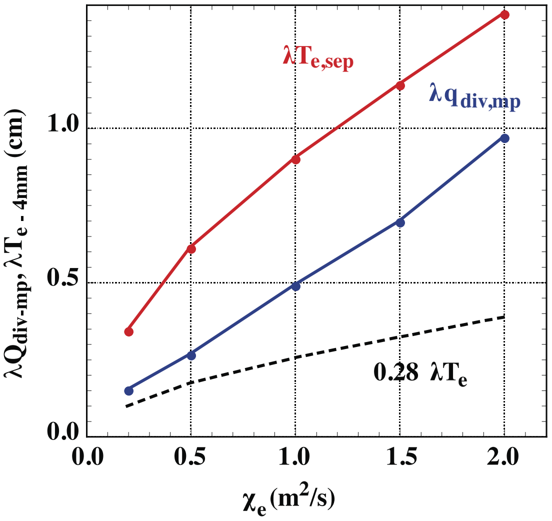

Fig. 3. Midplane scale lengths for electron temperature, λT_e, divertor heat flux, λQ, and value predicted from 2-point model (0.28 λT_e).

Moving beyond comparisons with 1D conduction, we have also examined the parameter dependence of the divertor heat flux profile width as predicted from the 2-point SOL model. Using the output from the full set of UEDGE parameter scans to determine $n_{e,sep}$, $T_{e,sep}$, and $\lambda_{q,mid}$, we evaluated the two-point model results [Eqs. (5) and (6)] to obtain $\lambda_{q,mid} \equiv \lambda_{q,\mathrm{2point}}$ for comparison. Midplane separatrix values for n_e and T_e were taken from UEDGE. As shown in Fig. 4, where we plot normalized $\lambda_{q,\mathrm{2point}}$ vs. $\lambda_{q,mid}$ from UEDGE, the conduction-limited two-point model reproduces the full 2D solution reasonably well. Note that, to account for geometrical factors missing from Eq. (5), all $\lambda_{q,\mathrm{2point}}$ values have been normalized by a single constant factor to match the UEDGE value at $\lambda_{q,mid} = 0.256$ cm. Note that, for $\lambda_{q,mid} \leq 0.4$ cm, the ratio of $T_{e,mid}$ to $T_{e,div}$ falls below 2, suggesting that the SOL should transition from the conduction-limited to sheath limited regime; this transition is much more evident when comparing UEDGE against Eq. (5), which is cannot be shown here due to space limitations.

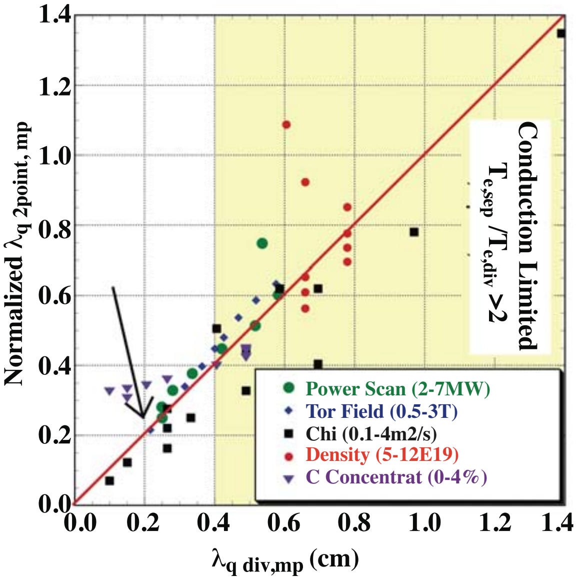

Fig. 4. Comparison between equivalent midplane heat flux profile as determined from conduction limited 2-point model [Eq. (5)] and 50 UEDGE divertor heat flux calculations mapped to midplane. Normalization for 2-point model data as indicated by arrow at y = 0.216).

VI. EFFECT OF SPATIALLY VARYING TRANSPORT COEFFICIENTS

It is widely recognized that assuming spatially uniform radial transport coefficients for particles and energy is likely an oversimplification for the scrape-off layer. Indeed, a radial variation in χ_e is often required to match simulation with experimental profiles in the SOL. It may be argued that SOL model validation will require a complete 2D map of the edge turbulence, but such measurements will not be available soon.

Here we explore how varying the poloidal distribution of the radial energy flux across the separatrix may affect both the divertor heat flux and midplane electron temperature profiles. We note that the larger surface area and compression of the outboard flux surfaces due to the Shafranov shift will peak radial transport at the outboard midplane significantly even with spatially uniform D and χ [2]. Giving the transport coefficients a ballooning character ($\chi \propto 1/B^2$ or even $1/B^3$) will lead to additional peaking of the radial transport at the outboard midplane $(B_T \propto 1/R)$. In all cases considered, the radial energy flow (W/m^2) is peaked at the outboard midplane $(\theta = 270°)$, with half the total power coming out within a full-width at half-maximum varying from ±50° (uniform $\chi = 0.5\ m^2/s$) to ±40° ($\chi \propto 1/B^3$, $0.18 \leq \chi \leq 1.5\ m_2/s$).

Poloidal peaking of the radial transport acts in the same manner as reducing a spatially uniform transport coefficient. In effect, radial transport is turned down everywhere except in one section of the SOL, and turning down χ leads to a narrower heat flux profile. Thus, if data is only available at midplane and divertor locations, it appears extremely hard to see any measurable difference in basic SOL properties resulting from poloidally non-uniform transport coefficients. Figure 5 compares computed midplane electron temperature profiles and divertor heat flux profiles for two cases having nearly the same field-line average $\chi_{ave} = (1/L_{||}) \int \chi(\ell) d\ell_{||}$ but very different form for χ: 81bb has uniform D, $\chi = 0.5\ m^2/s$ and ii has $\chi \propto 1/B^3$ with $\chi_{ave} = 0.49\ m^2/s$. The differences between the profiles are smaller than variations in typical DIII-D data.

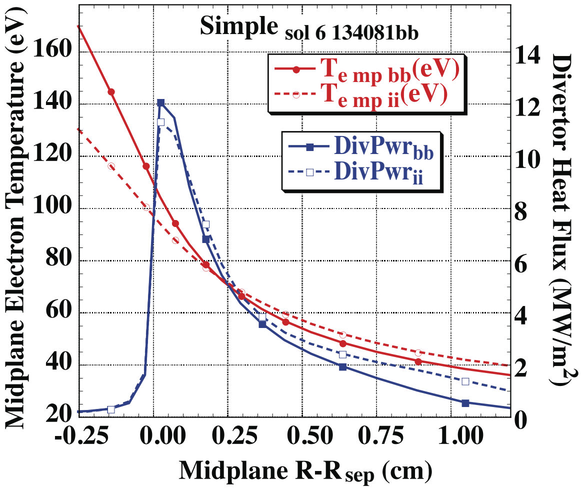

Fig. 5. Comparison of midplane electron temperature profiles and outer divertor heat flux profiles for case ii: uniform $\chi = 0.5\ \mathrm{m}^2/\mathrm{s}$ and case bb: $\chi \propto 1/\mathrm{B}^3$ with $\chi_{ave} = 0.49\ \mathrm{m}^2/\mathrm{s}$.

VII. CONCLUSIONS

This work reemphasizes that physics validation of the tokamak scrape-off layer physics requires application of comprehensive 2D analysis tools to make quantitative comparisons between midplane and divertor parameters. Using midplane (“upstream”) temperatures near the separatrix or temperature scale length coupled with 1D or “2-point” models to predict the peak divertor heat flux and profile widths can introduce significant systematic error unless the models are calibrated by a full 2D calculation. Further uncertainties will almost certainly arise when impurity transport, detachment physics, and particle drifts are added to the problem. For quantities of interest such as the divertor heat or particle flux, parameter variations and cross-tokamak comparisons should focus on these quantities, mapped back to the midplane to account for topological considerations, rather than introducing additional complexity by relating data via secondary quantities.

The weak dependence of divertor heat flux and midplane temperature profiles on the poloidal variation of radial transport coefficients suggests that validating SOL models by aiming forever more comprehensive diagnostic coverage around the boundary may be of limited value. On the other hand, the robustness of the basic scaling obtained from the simple 2-point model should motivate increased emphasis on parameter variations to validate the physics of the scrape-off layer. The value of using 2D simulation tools to explore the physics of the scrape-off layer and to identify and motivate new diagnostics and experiments cannot be overemphasized.

REFERENCES

[1]. T.D. Rognlien, *et al.*, Contrib. Plasma Phys. **34**, (1994) 362, and T. Rognlien, *et al.,* J. Nucl. Mater. **196-198** (1992) 347.

[2] G.D. Porter, *et al.*, Phys. Plasmas **3** (1996) 1967-1975.

[3] G.D. Porter, *et al.*, Phys. Plasmas, **7** (2000), 3663-3690.

[4] G.D. Porter, *et al.*, Fusion Sci. Technol. **48** (2005) 1127-1140.

[5] C.S. Pitcher, *et al,*, Plasma. Phys. Control. Fusion **39** (1997) 779-930.

[6] P. Stangeby, The Plasma Boundary of Magnetic Fusion Devices, Institute of Physics Publishing, Bristol and Philadelphia, 2000.

[7] R. Goldston, Phys. Plasmas **17**, (2010) 012503.

ACKNOWLEDGMENT

This work was supported by the U.S. Department of Energy under DE-FC02-04ER54698 and DE-AC52-07NA27344.